

CGC-Net: Cell Graph Convolutional Network for Grading of Colorectal Cancer Histology Images

Yanning Zhou, Simon Graham, Navid Alemi Koohbanani, Muhammad Shaban, Pheng-Ann Heng and Nasir Rajpoot

Presented by: Vasundhara Acharya

RIN:662018540

Department of Computer Science

Rensselaer Polytechnic Institute

3rd November, 2022

- 1 Introduction
- 2 Literature Survey
- 3 Problem Statement
- 4 Research questions
- 5 Methodology
- 6 Proposed Work: Methodology, Results and Conclusion

Introduction

- Colorectal cancer is a disease in which cells in the colon or rectum grow out of control
- It is the 3rd most cancer worldwide affecting both men and women [1]
- Around 90 % of CRCs is Adenocarcinomas (CRA).
- It is a type of cancer that starts in the large intestine
- Divided into two types: Low grade and High grade
- Low grade has well-differentiated carcinomas
- High grade has poorly differentiated carcinomas
- Grading CRA is crucial

- Automatic methods have been introduced in field of pathology to assist in grading of various types of cancers
- Tissue samples are digitized with scanner to create Whole slide Images (WSI).
- Digital signatures within the tissue help in cancer prognosis and assist clinical practices.
- Existing patch-based approaches lack interpretability and depend on images' resolution.
- To overcome these, the paper proposed an approach to extract cellular interactions in the form of a graph along with tissue structure.
- The extracted features are then fed to graph-based models to achieve the cancer grading.

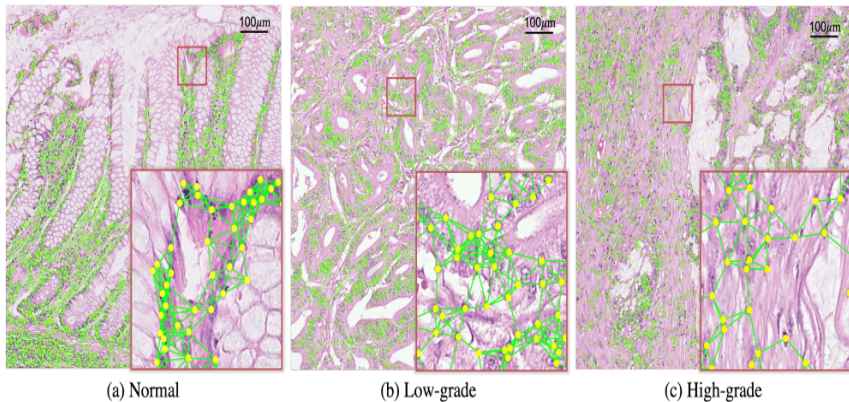


Figure: Typical cell graphs from (a) normal, (b) low-grade and (c) high grade images. The green lines represent the edges and the yellow dots represent the nuclei (graph nodes).

Literature Survey: Patch-based approaches

- Araújo et al. [2] proposed an approach to classify breast cancer histology images using a patch-based approach.
- They divided the original image into twelve contiguous non-overlapping patches.
- The patch class probability was computed using the patch-wise trained CNN and CNN+SVM classifiers.
- An accuracy of 83.3% for carcinoma/non-carcinoma was achieved.
- Coudray et al. [3] trained a deep convolutional neural network (inception v3) on whole-slide images of lung cancer obtained from The Cancer Genome Atlas.
- They broke the WSI into 512×512 patches and achieved an accuracy of 85.6%

Literature Survey: Cell Graphs

- Demir et al. [4] constructed augmented cell-graphs (ACG), from low-magnification tissue images of brain.
- Node represented cell cluster and edge described interaction.
- Trained neural networks with edge establishing features and global metrics.
- This approach achieved a sensitivity of 98.15 % in brain cancer classification.
- Bilgin et al.[5] proposed Cell-Graph Mining for Breast Tissue Modeling and Classification.
- Extracted graph features such as node degree, clustering coefficient, eccentricity, closeness etc to form feature set
- SVM achieved an accuracy of 81.8 % with the above feature set.

- Wang et al. [6] found that intricate spatial distribution information of the tumor microenvironment is informative for the prediction of the survival of Gastric cancer patients.
- Maximum effective distance was kept as 20m between immune and tumor cells while building the graph.
- GNN model could effectively capitalize on useful patterns generated by Cell-Graphs and achieved an ROC of 0.904 ± 0.012 for the classification.

Problem statement

- Computational techniques for automatic quantification and assessment of the tissue by considering the WSI have been increasing.
- To cope with the enormous size of WSIs, the researchers divide the images into patches.
- There is an inherent trade-off between the resolution of each image patch and the context provided.
- Features learned by the convolutional network may lack an interpretable correspondence to the tissue morphology and glandular structure.
- To overcome these drawbacks, nuclear features along with their cellular interactions in the form of a graph are necessary to capture cell-level information and the overall tissue micro-architecture

Research Questions

- Is there a significant relationship between interactions between the cells in the graph and actual biological interaction?
- Is the intricate spatial information of the cells obtained from cell graphs enough to grade cancer?

Methodology: Dataset Description

- CRC dataset [7] consisting of 139 images taken from WSIs with an average size of 4548×7520 at $20\times$ magnification is used
- Patches with a size of 1792×1792 pixels are utilized for cell graph construction.

Samples from the dataset

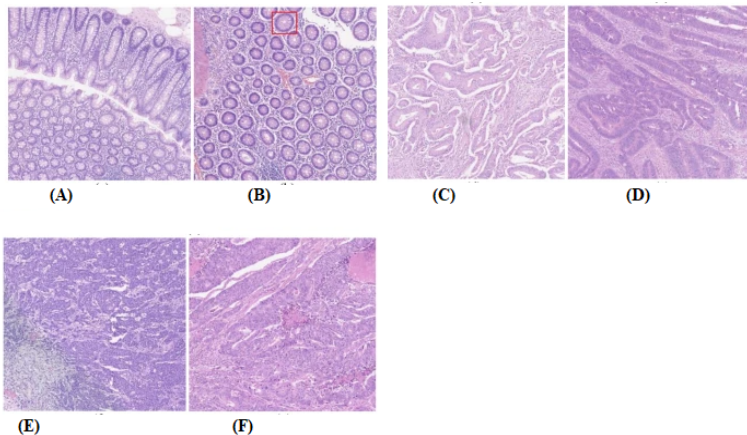


Figure: (A) and (B). **Normal tissue.** (C) and (D). **Low grade tumor tissue.** (E) and (F). **High grade tumor tissues**

- A graph is defined as $G = (V, E)$, which consists of a node set V with d -dimensional node features $x_i \in \mathbb{R}^d$ for $i \in V$ and edge set F_j , where $e_{i,j} = (i, j) \in F_j$ denotes an edge.
- An adjacency matrix $A \in \mathbb{R}^{n \times n}$ has non-zero entry $A_{ij} > 0$ if $e_{ij} \in E$.
- Nuclei are regarded as the nodes and the potential cellular interactions as edges of the graph

- To construct the graph, the following steps are involved:
 - Nuclear instance segmentation to extract node features
 - Representative node sampling to remove redundancy in the graph
 - Graph edge configuration to define potential cellular interactions

Nuclei extraction and Node sampling

- The authors utilized CIA-Net [8] to extract the nuclei from the images.
- It uses both nuclei level and contour level information to efficiently extract nuclei even in presence of clusters.
- Farthest Point Sampling (FPS) method is employed to choose a subset of nuclei, where each nucleus has the farthest distance to the selected nuclei collection.
- b-ratio of nuclei are sampled randomly and added to the subset to prevent overfitting.

- Edge is defined as the potential interaction between two nuclei.
- The cells with a smaller Euclidean distance are more likely to interact.
- Maximum degree of each node is set to K (10 in the proposed paper)
- Adjacency matrix is written as :

$$A_{ij} \begin{cases} 1 & \text{if } j \in KNN(i) \text{ and } D(i, j) < d \\ 0 & \text{otherwise.} \end{cases}$$

$D(\cdot, \cdot)$ denotes Euclidean distance.

Example

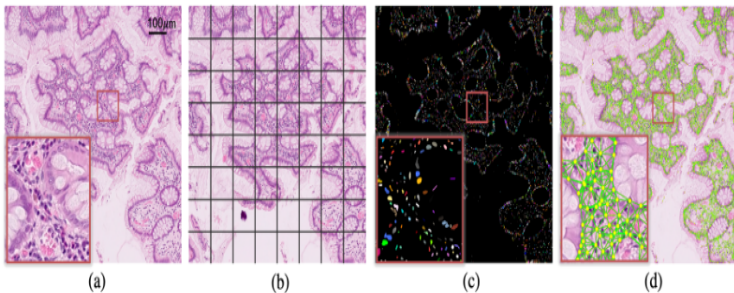
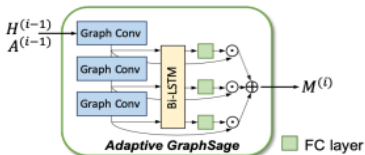
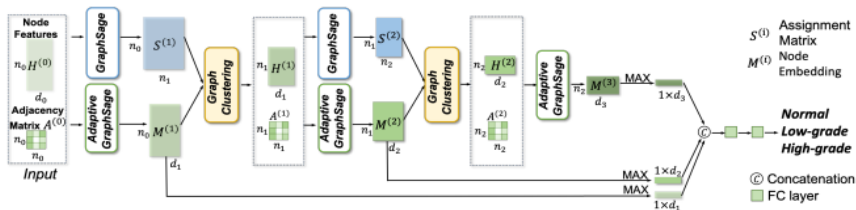


Figure: (a). Tissue sample. (b). Tiles on the image. (c). Nuclei extracted using the CIA-Net. (d). Cell graph overlaid on the image.

Features	Features
Number of Nodes	Number of edges
Nuclei position (Centroid)	GLCM Contrast
GLCM dissimilarity	Mean Intensity
Nuclei Area	Orientation
Major Axis length	Minor Axis Length
Convex hull area	Eccentricity
Perimeter	Solidity

Table: Feature set

Graph Convolutional Network



Structure of the CGC-Net

Figure: CGC-Net

A typical graph convolution operation can be written as:

$$h_i^{(l)} = \sigma \left(W^{(l)} \cdot \text{Agg} \left\{ h_j^{(l-1)}, \forall j \in \tilde{N}(i) \right\} \right)$$

Where $h_i^{(l)} \in \mathbb{R}^d$ denotes the hidden features, $W^{(l)}$ is learnable weight

- GraphSage assigns same weights for all node embeddings (it is not adaptive)
- Adaptive GraphSage assigns weights to the node embeddings according to local structure
- K graph convolutions are stacked to capture information from K nodes
- $h_v^{(1)}, h_v^{(2)}, \dots, h_v^{(k)}$ are fed to bi-directional LSTM to generate embedding for each feature.
- These concatenated embeddings are sent to Softmax to get importance score.
- Each node is then represented by weighted sum of multi-level features.

Graph Clustering

- GNN architectures is that they are inherently flat
- They propagate information across the edges of the graph
- Unable to infer and aggregate the information in a hierarchical way
- Consider an example of graph with organic molecules.
- Graph Clustering module helps to capture this information

Results

Node Features	GC	Sampling	Patch Accuracy	Image Accuracy
Appearance & Spatial	<i>GS</i>	Fuse	89.42 ± 1.68	96.28 ± 2.82
Appearance & Spatial	<i>AGS</i>	Random	88.11 ± 2.47	93.25 ± 1.94
Appearance & Spatial	<i>AGS</i>	Farthest	89.47 ± 2.71	96.28 ± 1.03
Spatial	<i>AGS</i>	Fuse	69.50 ± 3.56	86.63 ± 4.67
Appearance	<i>AGS</i>	Fuse	89.68 ± 2.28	97.00 ± 1.10
Appearance & Spatial	<i>AGS</i>	Fuse	91.60 ± 1.26	97.00 ± 1.10

Figure: Average patch-level accuracy and image-level accuracy on CRC dataset. GC represents the graph convolution method, where GS and AGS denote GraphSage and Adaptive GraphSage respectively. Sampling represents the nuclei sampling strategy.

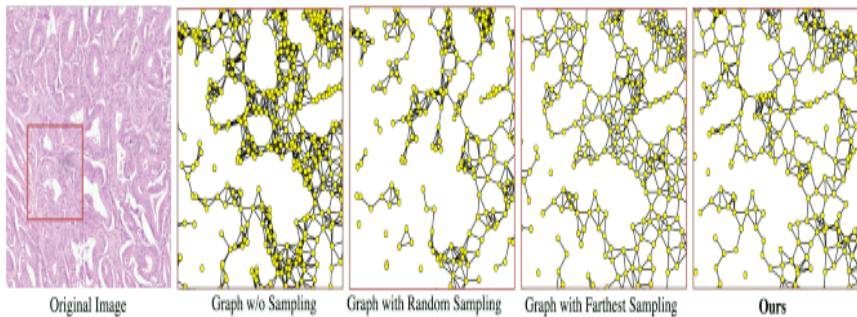


Figure: Comparison of different node sampling strategies

Method	Image Accuracy
BAM-1 [2]	87.79 \pm 2.32
BAM-2 [2]	90.66 \pm 2.45
Context - G [42]	89.96 \pm 3.54
ResNet50 [26]	92.08 \pm 2.08
MobileNet [27]	92.78 \pm 2.74
InceptionV3 [46]	91.37 \pm 3.55
Xception [8]	92.09 \pm 0.98
CA-CNN [41]	95.70 \pm 3.04
Ours	97.00 \pm 1.10

Figure: Comparison with state-of-the-art on CRC dataset.

Conclusion

- Nuclei sampling strategy helped to reduce computational redundancy
- Proposed approach accurately classified cancer by modeling the tissue micro environment.
- Model trained with local interactions and cell appearance features outperformed state-of-the-art models.

- Positive aspects:
 - Fascinating idea of mapping the real-time interaction between the cells in the tissue to form a cell graph
 - Adaptive architecture of GraphSage that has the capability to aggregate multi-level feature embedding
- Negative aspects:
 - Focuses more on the appearance features rather than the features captured via the interaction in cell graphs.
 - Paper lacks qualitative analysis

Proposed Work: Tuberculosis Prediction from Lung Tissue Images of Diversity Outbred Mice using Enhanced Cell Graph Neural Network

- Tuberculosis (TB) is diagnosed in 10 million human patients and causes 1.5 million deaths each year.
- Mycobacterium tuberculosis causes pulmonary tuberculosis typically restricted to the lungs.
- Existing approaches fail to use the entire image (uses only patches).
- Cell-graphs extracted from entire lung tissue images improves the assessment of the link between the spatial patterns and end prognosis of Tuberculosis.

Table: Variations from Reference Paper

Sections	Reference Paper	Proposed Method
Aim	Grading of Colorectal Cancer Histology Images	Classification of Tuberculosis from Lung Histopathology Images
Number of Labels used for Grading/Classification	3-Normal, Low-grade, High-grade	2 -Infected and Uninfected
Dataset	Colorectal cancer dataset (CRC)	Mycobacterium tuberculosis dataset
Subjects	Humans	Diversity Outbred Mice
Dataset Size	38 Whole slide images	40 Whole slide images
Edge weight determining algorithm	K-Nearest Neighbor	Euclidean Distance and Giant Connected Component

Table: Variations from Reference Paper

Sections	Reference Paper	Proposed Method
Features extracted	Mostly Appearance features and some spatial features	Graph Features and Appearance features
Algorithms Employed for Grading/Classification	Context-Aware-CNN, BAM, ResNet-50, Inception V3, Xception, MobileNet and Adaptive GraphSage	Random Forest, SVM, ANN, GCN, GAT, GraphSage
Performance Metrics	Image Level and Patch level accuracy	Node level accuracy, Graph level accuracy, Precision, Recall, F1 score

Methodology: Dataset Description

- WSI of Mycobacterium infected lung tissues obtained from diversity outbred mice
- Stain: Modified Ziehl-Neelson with carbol fuchsin.
- Size: 38 WSI
- Each of the whole slide images consist of AFB and nuclei.
- Gillian Beamer, Assistant Professor from Tufts University, performed the staining and initial analysis of whole slide images.
- The locations of individual nuclei and AFB are found using a novel machine learning model.
- Format of image :SVS

- PyTorch and Weka for training and classification
- OpenSlide for image processing
- QuPath tool for visualization
- DeepSNAP: library to assist efficient deep learning on graphs
- Deep Graph Library (DGL) : For easy implementation of graph neural network model family
- Optuna: For hyperparameter optimization

- Only the X coordinate, Y coordinate and node labels are extracted
- The centroid X and Y coordinates are given in micrometer.
- These coordinates are converted to pixel values for further processing.

Samples

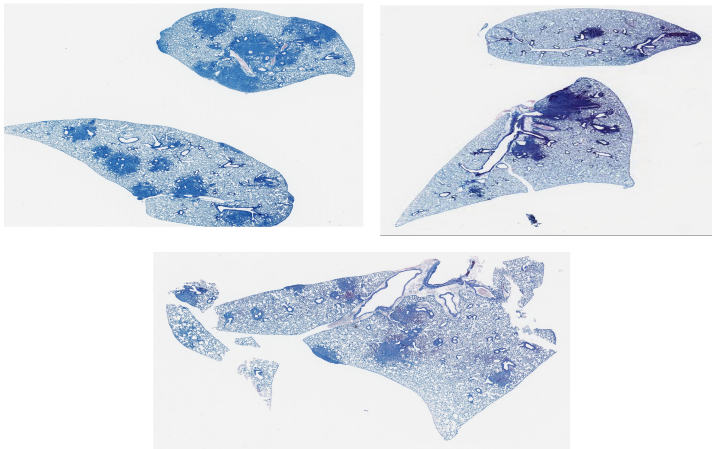


Figure: Sample images of WSI

Detailed Stages

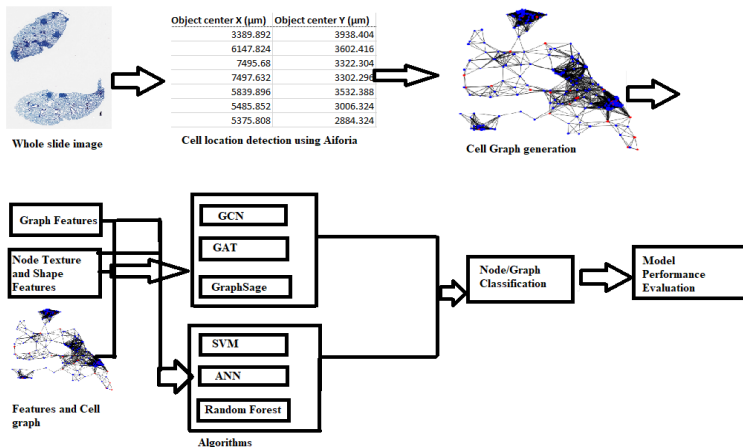


Figure: Stages in the proposed approach

- Construct the cell graph by utilizing the cell centroid values
- Extract local and global features from the graphs
- Extract appearance features from the images
- Employ the cell graph along these feature vectors to train various models.
- Classify the entire graph as infected/uninfected
- Classify each node as a Nuclei/AFB

Cell Graph Construction

- Nodes in the cell graph indicate Nuclei/AFB
- Edges indicate the interaction between these cells
- Edge weights are the euclidean distance between the cells
- Threshold is computed such that the giant connected component has atleast 95 % of the cells
- Edges are eliminated if the edge weight exceeds this threshold value.

Adjacency Matrix

Adjacency matrix is written as :

$$A_{ij} \begin{cases} 1 & \text{and } D(i,j) < d \\ 0 & \text{otherwise.} \end{cases}$$

$D(\cdot, \cdot)$ denotes Euclidean distance. d denotes the threshold computed

Example Cell Graph

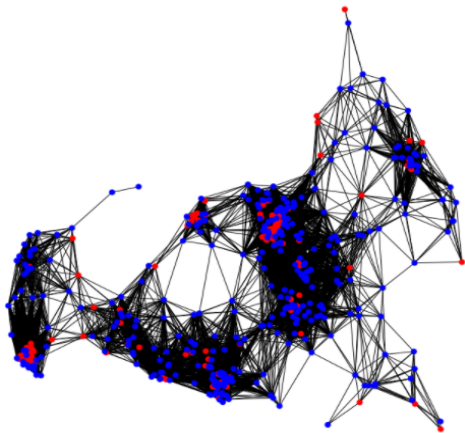


Figure: Cell graph of slide number 151. The red nodes indicate AFB. The blue nodes indicate Nuclei. The black lines are the edges indicating the interaction. Edge threshold was 130.

Hypothesis

Cells in the infected lung tissue will interact more among themselves than the cells in the uninfected lung tissue.

Proof: Less number of edges are seen in graph obtained from uninfected lung tissue

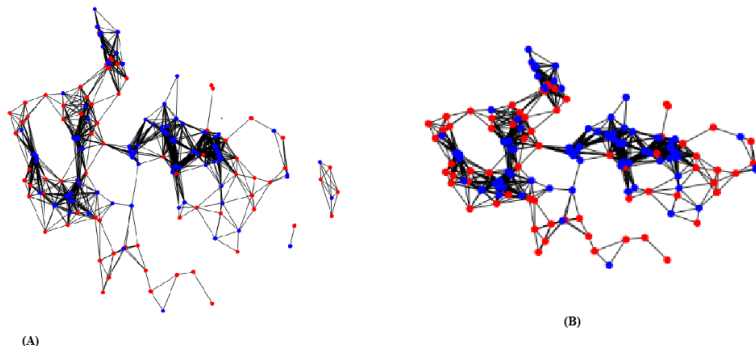


Figure: (A). Cell graph of uninfected slide with id 189. (B). Giant connected component with 189 nodes and 1677 edges. The ratio of nodes to edges is almost 1:8.

More number of edges are seen in graph obtained from infected lung tissue

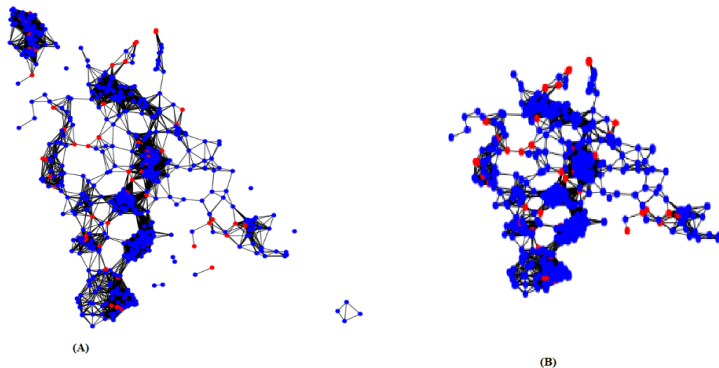


Figure: (A). Cell graph of infected slide with id 159. (B). Giant connected component with 603 nodes and 11179 edges. The ratio of nodes to edges is almost 1:19. Edge threshold was 185.

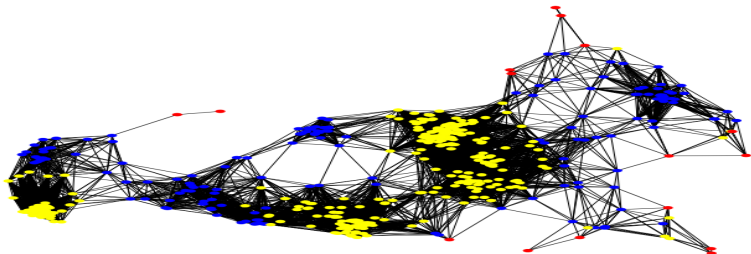


Figure: Slide 151 with nodes colored degree wise. Nodes with red color have a degree of less than 10. Nodes with blue color have degree between 10 and 50. Nodes with yellow color have degree greater than 50.

Overlay of the cell graph on original image for visualization

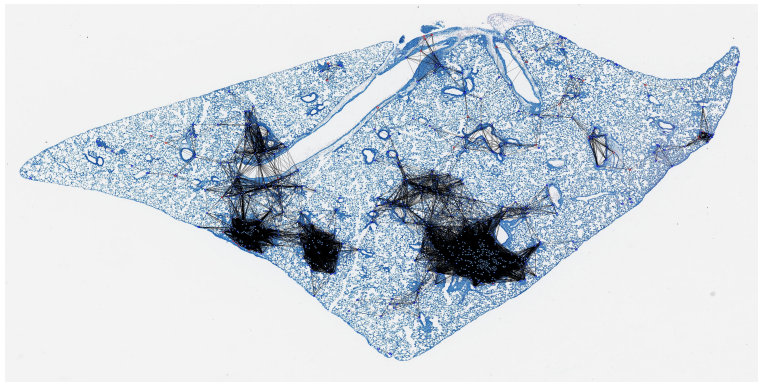


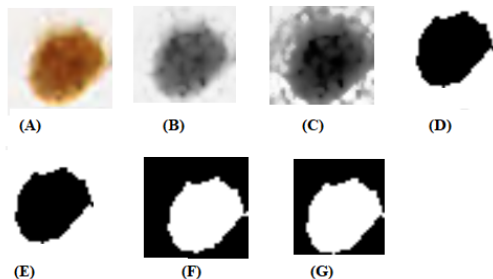
Figure: Overlay of cell graph on original image obtained on slide number 182.

Graph Features

Simple Metrics:	Number of Nodes: Number of cells in the tissue.
	Number of Edges: Number of hypothesized interactions
Distance Based Metrics	Eccentricity of a Node
	Diameter
	Radius
	Closeness of a Node
	Number of central points
Connectedness and Cliquishness Measures:	Average Degree
	Clustering Coefficient of a Node
	Giant Connected Component Ratio
	Percentage of Isolated Points
	Percentage of End Points
Spectral features	Trace of adjacency
	Energy of adjacency
	Number of zeros normalized Laplacian
	Lower Slope_L
	Number of ones normalized Laplacian
	Upper Slope_L
	Trace of Laplacian
	Energy of Laplacian
	Lower Slope_L
	Upper Slope_L
	Number of ones Adjacency
	Number of zeros Adjacency

Local structural features	Degree of the i th representative vertex
	Clustering coefficient C
	Eccentricity of the i th representative vertex
	Closeness
	Betweenness
	Mean knn distance of the i th representative
	Skewness of the knn of i th representative
	Kurtosis of the knn of the i th representative
	Mean edge length of the i th representative
	Skewness of the edge length of the i th representative
Kurtosis of the knn of the i th representative	
Local and Global Overlap features	simrank similarity
	Salton Index
	Hub Promoted index
	Hub Depressed Index
	Sorenson index
	Katz centrality

Node appearance features extraction using OpenSlide



(A). Original image from the whole slide image. (B). Grayscale conversion. (C). Histogram equalized image. (E). Conversion to Binary using Otsus and binary threshold. (F). Morphological open with ellipse (2*2). (G). Morphological erode with ellipse (1*1). (H). Hole filled final image using plantcv

Table: Appearance Features

Features	Features
Mean Intensity	Minor axis
Diameter	Perimeter
Major axis	Area
Contrast	dissimilarity
Correlation	Energy
cluster	entropy
Homogeneity	Variance
ASM_value	Circularity
Mean_convex_hull	SD_convex_hull
Centroid X	Centroid Y

- Support Vector Machine (SVM)
- Random Forest (RF)
- Artificial Neural Network (ANN)
- Simple Graph Convolutional Network (GCN)
- GraphSage: capable of representing and classifying previously unseen nodes with high accuracy
- Graph Attention Network (GAT): leverages attention over a node's neighborhood
- The entire dataset is split as 70 % training and 30 % test set.
- Number of graphs :15
- Training set nodes : 11215, Test set nodes: 4807

Results of Random Forest with Graph Features

- Best hyperparameters obtained:
- `N_estimators:100`
- `min_samples_split=6`
- `min_samples_leaf=3`
- `max_depth =40`
- `max_features=sqrt`
- `Bootstrap='False'`

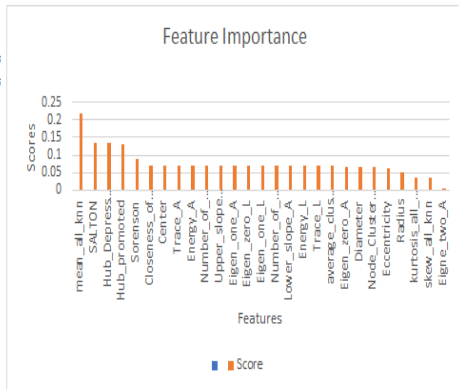
=== Summary ===

Correctly Classified Instances	4336	89.7723 %
Incorrectly Classified Instances	494	10.2277 %
Kappa statistic	0.7438	
Mean absolute error	0.1682	
Root mean squared error	0.2771	
Relative absolute error	40.334 %	
Root relative squared error	61.0086 %	
Total Number of Instances	4830	

=== Confusion Matrix ===

a	b	<-- classified as
1081	322	a = AFB
172	3255	b = Nuclei

(A)



(B)

Figure: (A). Confusion matrix with test accuracy of 89.7%. (B) Feature importance (Local structural features are more important than global features)

Explanation of features with highest importance

- Mean of all K-nearest Neighbors:

$$\frac{\sum D(A, s(A))}{|S(A)|}$$

here, $s(A)$ denotes all the neighbors of node A.

- Salton

$$S_{(a,b)} = \frac{2|S(A) \cap S(B)|}{\sqrt{d(A) + d(B)}}$$

$d(a)$ and $d(b)$ indicate the degree of nodes A and B respectively.

- Hub Depressed Index:

$$s_{\text{HDI}}(u, v) = \frac{|S(u) \cap S(v)|}{\max\{|S(u)|, |S(v)|\}}$$

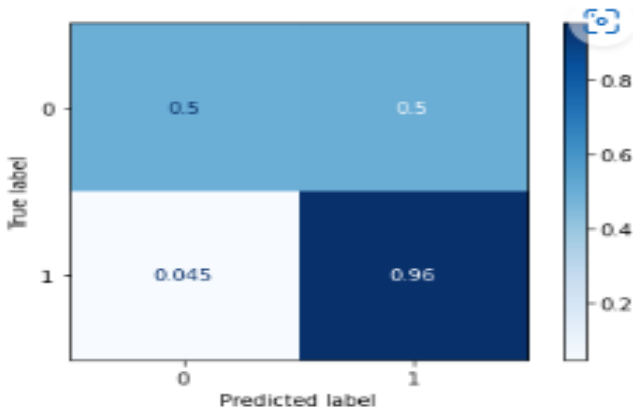
normalize the overlap between neighbors of two nodes based on the degrees of the nodes by focusing on the node with higher degree

- Sorenson Index:

$$S_{(a,b)} = \frac{2|S(a) \cap S(b)|}{d(a) + d(b)}$$

Results with SVM

- C:1000
- Gamma=0.01
- Kernel=RBF



Model accuracy: 0.817429103705237

Figure: Confusion matrix with test accuracy of 81.74%.

Results with ANN

- Batch size:20
- Epochs :200
- Optimizer :Adam

	precision	recall	f1-score	support
0	0.52	0.88	0.65	1445
1	0.93	0.66	0.77	3386
accuracy			0.72	4831
macro avg	0.72	0.77	0.71	4831
weighted avg	0.80	0.72	0.73	4831

Figure: Confusion matrix with test accuracy of 72%.

Results with GraphSage

Best hyperparameters chosen:

- Hidden dimensions :20
- Dropout=0.5
- Learning rate :0.0001
- Epochs:250
- Optimizer: Adam

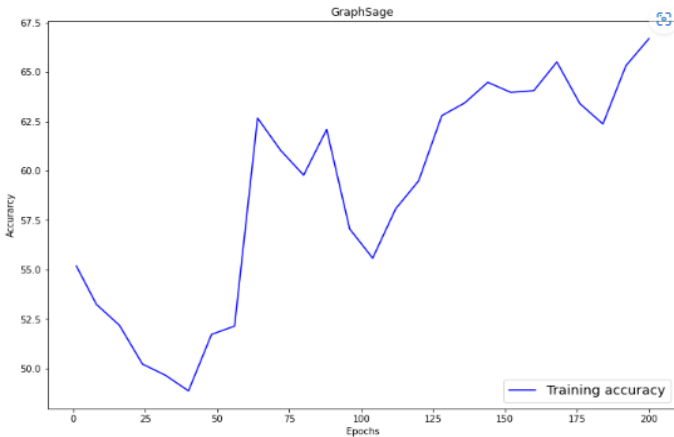


Figure: GraphSage performance. Train accuracy is 66.69%. Test accuracy is 68%

Results with GCN

- Hidden dimensions :34
- Dropout=0.32177261465837625
- Learning rate :0.0001
- Epochs:250
- Optimizer: Adam

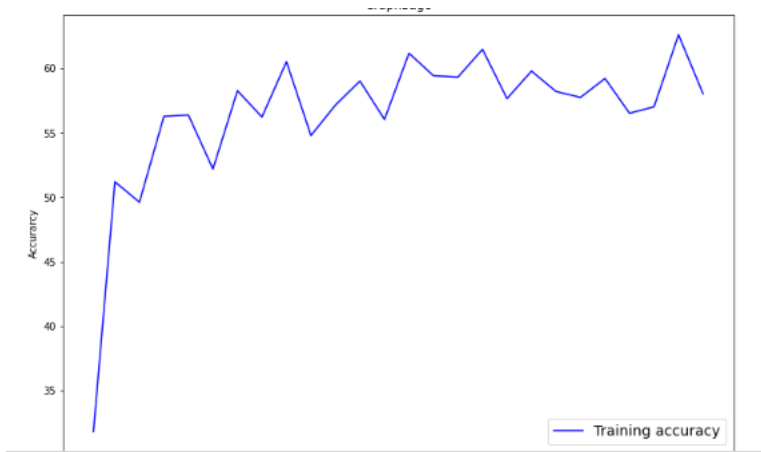


Figure: GCN performance. Train accuracy is 58.03% (much less than GraphSage). Test accuracy is 42.5%

Results with GAT

Hidden dimensions :34

Dropout=0.5

Learning rate :0.001

Epochs:250

Optimizer: Adam

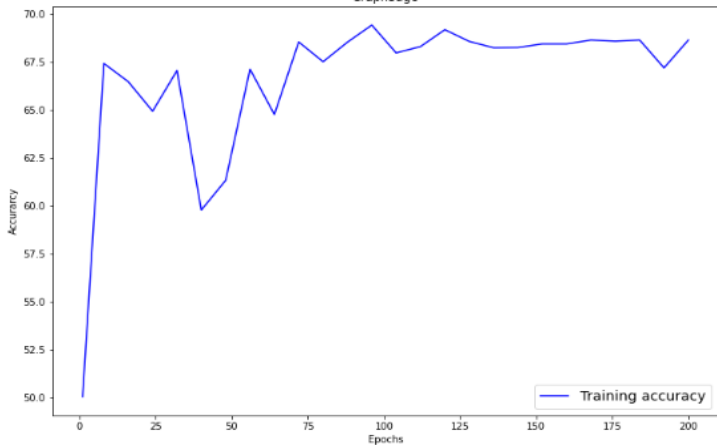


Figure: GAT performance. Train accuracy is 68.63%. Test accuracy is 68.8%

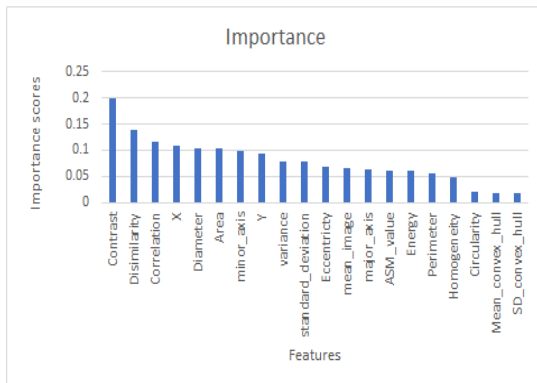
Summary of performance using graph features

Model	Accuracy (on test set)
Random Forest	89.7
SVM	81.74
ANN	72
GraphSage	68
GAT	68.8
GCN	42.5

Results with Random Forest

```
=== Confusion Matrix ===  
  
  a   b  <-- classified as  
1007 432 |   a = AFE  
 246 3122 |   b = Nuclei
```

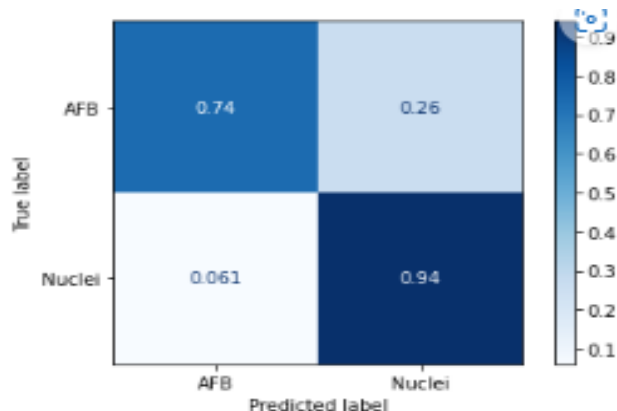
(A)



(B)

Figure: Random Forest Performance. (A). Confusion matrix on test set with a test accuracy of 85.89% (B). Feature importance

Results with SVM



Model accuracy: 0.8778864156438527

Figure: SVM Performance: Test accuracy obtained was 87.78%

Results with ANN

	precision	recall	f1-score	support
0	0.85	0.68	0.76	1418
1	0.88	0.95	0.91	3389
accuracy			0.87	4807
macro avg	0.86	0.82	0.84	4807
weighted avg	0.87	0.87	0.87	4807

Figure: ANN Performance: Test accuracy obtained was 87%

Results with GraphSage

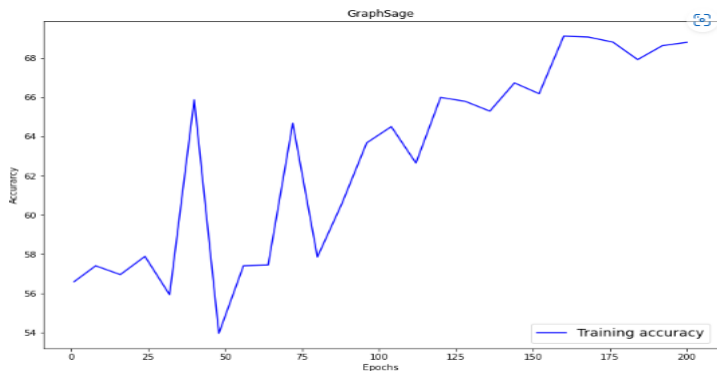


Figure: Training accuracy is 68.8%. Test accuracy is 40.70%

Results with GAT

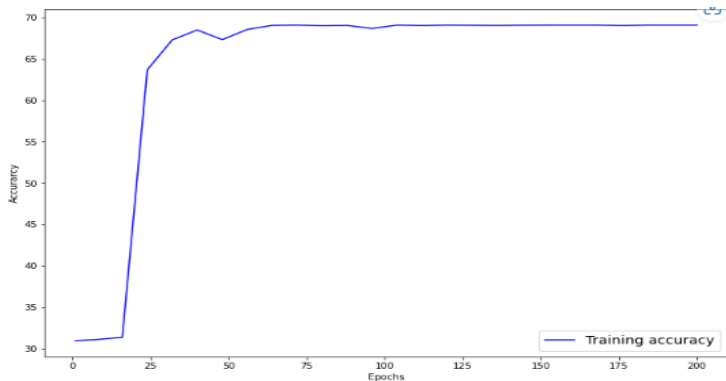


Figure: Training accuracy is 69%. Test accuracy is 67%

Results with GCN

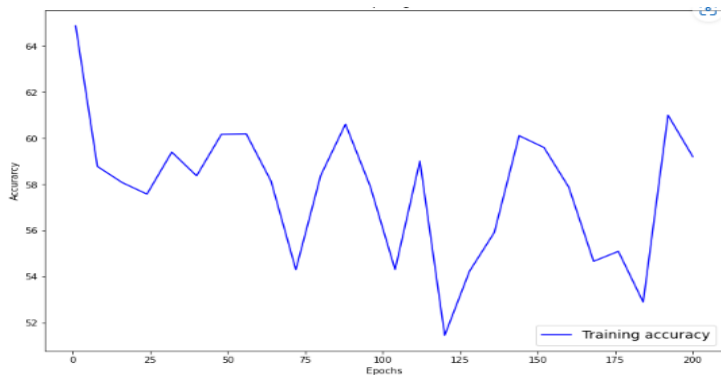


Figure: Training accuracy is 59.2%. Test accuracy is 58.14%

Summary of performance using appearance features

Model	Accuracy (on test set)
Random Forest	85.89
SVM	87.78
ANN	87
GraphSage	40.7
GAT	67
GCN	58.14

Graph Classification results

- Infected graph:13, Uninfected graph:2
- Training graphs:10, test graphs :5

Table: Model performance (in accuracy (percent)) for graph classification

Model	Training_Accuracy	Test_Accuracy
GCN	88.89	50
GAT	92.31	99
GraphSage	92.21	99

Conclusion





- Cell graphs improved the assessment of the link between the spatial patterns and the end prognosis of Tuberculosis.
- Features extracted from graphs were beneficial in the classification of lung images into infected/uninfected
- Appearance features assisted the model in classifying the nodes as either Nuclei/AFB.
- Local graph features also played a vital role in node classification
- Graphs obtained from infected slides were denser than the graphs obtained from uninfected slides.

Any Questions?

Questions?

Thank You

Thank You !

-  “Colorectal cancer statistics,” Apr 2022. [Online]. Available: <https://www.wcrf.org/cancer-trends/colorectal-cancer-statistics/>
-  T. Araújo, G. Aresta, E. Castro, J. Rouco, P. Aguiar, C. Eloy, A. Polónia, and A. Campilho, “Classification of breast cancer histology images using convolutional neural networks,” *PloS one*, vol. 12, no. 6, p. e0177544, 2017.
-  N. Coudray, P. S. Ocampo, T. Sakellaropoulos, N. Narula, M. Snuderl, D. Fenyö, A. L. Moreira, N. Razavian, and A. Tsirigos, “Classification and mutation prediction from non–small cell lung cancer histopathology images using deep learning,” *Nature medicine*, vol. 24, no. 10, pp. 1559–1567, 2018.
-  C. Demir, S. H. Gultekin, and B. Yener, “Augmented cell-graphs for automated cancer diagnosis,” *Bioinformatics*, vol. 21, no. suppl_2, pp. ii7–ii12, 2005.
-  C. Bilgin, C. Demir, C. Nagi, and B. Yener, “Cell-graph mining for breast tissue modeling and classification,” in *2007 29th Annual*

International Conference of the IEEE Engineering in Medicine and Biology Society. IEEE, 2007, pp. 5311–5314.



Y. Wang, Y. G. Wang, C. Hu, M. Li, Y. Fan, N. Otter, I. Sam, H. Gou, Y. Hu, T. Kwok *et al.*, “Cell graph neural networks enable the precise prediction of patient survival in gastric cancer,” *NPJ precision oncology*, vol. 6, no. 1, pp. 1–12, 2022.



R. Awan, K. Sirinukunwattana, D. Epstein, S. Jefferyes, U. Qidwai, Z. Aftab, I. Mujeeb, D. Snead, and N. Rajpoot, “Glandular morphometrics for objective grading of colorectal adenocarcinoma histology images,” *Scientific reports*, vol. 7, no. 1, pp. 1–12, 2017.



Y. Zhou, O. F. Onder, Q. Dou, E. Tsougenis, H. Chen, and P.-A. Heng, “Cia-net: Robust nuclei instance segmentation with contour-aware information aggregation,” in *International conference on information processing in medical imaging*. Springer, 2019, pp. 682–693.